

Rate-Splitting Multiple Access for Cell-Free ISAC Massive MIMO systems

Mario R. Camana, *Member, IEEE*, Carla E. Garcia, *Member, IEEE*, and Inkyu Lee, *Fellow, IEEE*

Abstract—This paper investigates rate-splitting multiple access (RSMA) in a cell-free massive multi-input multi-output (MIMO) system with integrated sensing and communication (ISAC). In this system model, we consider the maximization of the minimum rate subject to radar sensing constraints and a maximum power budget. A successive convex approximation based scheme is developed to solve the non-convex problem by optimizing the precoding vectors for radar and communication, as well as the common rate variables. Numerical results show the superior performance of the proposed RSMA method over conventional cell-free massive MIMO schemes under different scenarios with varying numbers of APs, antennas, and users.

Index Terms—Cell-Free massive MIMO, integrated sensing and communication (ISAC), rate-splitting multiple access (RSMA), transmit beamforming.

I. INTRODUCTION

Next generation wireless networks are envisioned for a wide range of applications such as vehicle-to-everything, smart manufacturing, smart homes, and remote sensing, which rely on robust and accurate sensing capabilities. To meet these demands, integrated sensing and communication (ISAC) has emerged as a promising technology that enables joint radar sensing and wireless communication using shared infrastructure and spectrum resources. This allows for efficient spectrum utilization and cost-effective deployment [1]–[4], and has inspired recent waveform designs [5].

The authors in [1] investigated the co-existence of radar and communication, demonstrating the benefits of shared deployment where all antennas are used for radar and downlink communication. In [2], a dedicated radar signal was designed to provide full degrees of freedom (DoF) for radar sensing, and the radar beampattern was optimized subject to signal-to-interference-plus-noise ratio (SINR) requirements at users. A new radar sensing design was proposed in [3] by maximizing the minimum beampattern gain. These works laid the foundation for ISAC systems but primarily focused on co-located MIMO architectures.

Recently, cell-free massive multi-input multi-output (MIMO) has attracted attentions as a promising technology to meet the

This work was supported in part by the National Research Foundation of Korea (NRF) grant funded by the Korea government (MSIT) under Grant RS-2022-NR070834, and in part by the Institute of Information and Communications Technology Planning and Evaluation (IITP) Grants by MSIT under Grant 2021-0-00467.

Mario R. Camana and Carla E. Garcia are with the Interdisciplinary Centre for Security, Reliability and Trust, University of Luxembourg, 4365 Luxembourg City, Luxembourg (e-mail: mario.camana@uni.lu, carla.garcia@uni.lu).

Inkyu Lee is with the School of Electrical Engineering, Korea University, Seoul 02841, Korea (e-mail: inkyu@korea.ac.kr).
(Corresponding author: Inkyu lee)

requirements of future networks [6]– [9]. In this system, a large number of access points (APs) are distributed geographically within an infrastructure, which are connected through backhaul links to a central processing unit (CPU), enabling coordinated transmission and reception. In [7], a cell-free massive MIMO system with multi-antenna APs was considered to maximize the total energy efficiency subject to a maximum transmit power at each AP. It was shown that cell-free massive MIMO can outperform conventional co-located massive MIMO.

On the other hand, rate-splitting multiple access (RSMA) has been introduced to mitigate multi-user interference in multi-antenna systems. The RSMA partially decodes interference and treats as noise by optimizing the information split between the common and private messages, where the common message is decoded by all users with the successive interference cancellation (SIC) procedure [10]. RSMA has proven to be an effective technology to improve spectrum and energy efficiency compared to traditional methods [10]– [16].

An overview of RSMA principles and applications is provided in [11]. In ISAC systems, RSMA has been recognized as a powerful interference management strategy [13], [14], capable of reducing both inter-user and sensing-communication interference. Specifically, the work [13] introduced RSMA’s dual-function interference mitigation, while the authors in [14] demonstrated RSMA’s superiority over conventional schemes such as non-orthogonal multiple access (NOMA) and space-division multiple access (SDMA). Prior research has investigated the integration of ISAC with cell-free massive MIMO [17], but without incorporating RSMA. While RSMA has been studied in ISAC [13], [14] and in cell-free massive MIMO systems [15], [16], its joint application within a cell-free ISAC framework remains unexplored. This integration introduces new challenges, including distributed interference management, coordinated beamforming across multiple APs, and joint optimization of radar and communication operations under power and beampattern constraints.

In this paper, motivated by the performance gains of RSMA in both ISAC systems and cell-free-MIMO networks, we propose a new approach based on the RSMA framework to more effectively manage interference between radar and communication functions, as well as among communication users, in a cell-free massive MIMO system with ISAC by optimizing the precoding vectors and power allocation. To the best of our knowledge, this is the first research which considers RSMA for ISAC in a cell-free massive MIMO system. The main contributions of this paper can be summarized as follows:

- In a cell-free ISAC massive MIMO system with RSMA, we aim to jointly optimize communication and radar

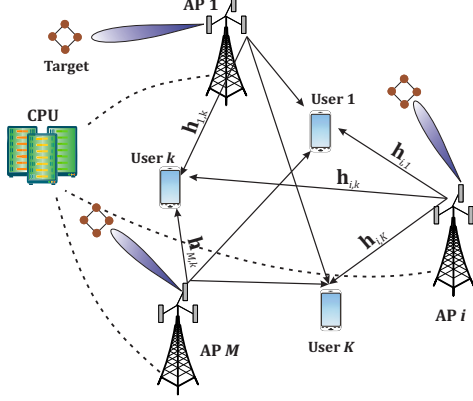


Fig. 1. Cell-free massive MIMO system with ISAC.

beamforming by maximizing the minimum rate of users under constraints on the minimum required beampattern gain, common rate decoding requirements, and maximum power budget.

- To address the formulated non-convex optimization problem, we propose a successive convex approximation (SCA)-based technique, which relies on tailored surrogate functions to optimize the precoding vectors for radar and communication, as well as the common rate variables.

Numerical results show that the proposed RSMA-based ISAC scheme achieves similar performance to RSMA without sensing operations and provides superior performance compared to conventional non-RSMA methods.

II. SYSTEM MODEL AND PROBLEM FORMULATION

We consider a cell-free massive MIMO system with ISAC as illustrated in Fig. 1. The system model consists of K single-antenna users, and M geographically distributed APs equipped with N antennas. We assume that each AP performs sensing for one target. The CPU executes the cooperation among APs through fronthaul links. The set of APs sends information-bearing signals along with a dedicated radar signal to carry out sensing and communication simultaneously.

Under the RSMA strategy, the message W_k intended for the k -th user is divided into a common part W_k^c and a private part W_k^p . The common parts of all messages are grouped together into the common stream s_0 by using a shared codebook and are decoded by all users, as illustrated in Fig. 2 for the i -th AP. Each private message W_k^p is encoded into an independent stream s_k ($k = 1, \dots, K$) to be decoded only by the k -th user. Let $\mathbf{p}_{i,0} \in \mathbb{C}^{N \times 1}$ and $\mathbf{p}_{i,k} \in \mathbb{C}^{N \times 1}$ be the precoder vectors at the i -th AP for the common stream and the private stream, respectively. Also, the dedicated radar signal s_R at the i -th AP is precoded by the precoder vector $\mathbf{p}_{i,R} \in \mathbb{C}^{N \times 1}$. Then, the transmit signal of the i -th AP is expressed as $\mathbf{x}_i = \mathbf{p}_{i,0}s_0 + \mathbf{p}_{i,R}s_R + \sum_{k=1}^K \mathbf{p}_{i,k}s_k$.

Thus, the received signal at the k -th user is obtained by

$$y_k = \sum_{i=1}^M \mathbf{h}_{i,k}^H \mathbf{p}_{i,0} s_0 + \sum_{i=1}^M \sum_{j=1}^K \mathbf{h}_{i,k}^H \mathbf{p}_{i,j} s_j + \sum_{i=1}^M \mathbf{h}_{i,k}^H \mathbf{p}_{i,R} s_R + n_k, \quad (1)$$

where $\mathbf{h}_{i,k} \in \mathbb{C}^{N \times 1}$ represents the channel vector from the i -th AP to the k -th user, and $n_k \sim \mathcal{CN}(0, \sigma_k^2)$ is the additive

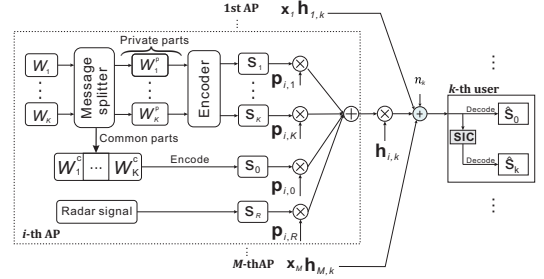


Fig. 2. RSMA transmission framework at the i -th AP.

noise at the k -th user. In RSMA, each user first decodes the common stream by treating all private streams as noise. Once the common stream is successfully decoded and canceled using the SIC procedure, each user then decodes its private stream.

Then, the SINR for the common stream s_0 at the k -th user is written by

$$\text{SINR}_k^c = \frac{\left| \sum_{i=1}^M \mathbf{h}_{i,k}^H \mathbf{p}_{i,0} \right|^2}{\sum_{k'=1, k' \neq k}^K \left| \sum_{i=1}^M \mathbf{h}_{i,k}^H \mathbf{p}_{i,k'} \right|^2 + \left| \sum_{i=1}^M \mathbf{h}_{i,k}^H \mathbf{p}_{i,R} \right|^2 + \sigma_k^2}. \quad (2)$$

Also, the SINR at the k -th private stream s_k is computed by

$$\text{SINR}_k^p = \frac{\left| \sum_{i=1}^M \mathbf{h}_{i,k}^H \mathbf{p}_{i,k} \right|^2}{\sum_{k'=1, k' \neq k}^K \left| \sum_{i=1}^M \mathbf{h}_{i,k}^H \mathbf{p}_{i,k'} \right|^2 + \left| \sum_{i=1}^M \mathbf{h}_{i,k}^H \mathbf{p}_{i,R} \right|^2 + \sigma_k^2}. \quad (3)$$

Thus, the achievable rates at the k -th user for the common and private stream are equal to $R_k^c = \log_2(1 + \text{SINR}_k^c)$ and $R_k^p = \log_2(1 + \text{SINR}_k^p)$, respectively. To ensure that the common stream s_0 is successfully decoded by all users, its maximum transmission rate cannot exceed $R_0 = \min\{R_1^c, \dots, R_K^c\}$. Since s_0 carries the users' sub-messages, R_0 is distributed among the users in proportion to the size of their respective sub-messages. Let r_k denote the common rate for the k -th user, representing the portion of R_0 allocated to transmit W_k^c such that $\sum_{k=1}^K r_k = R_0$.

For the precoder design of the private streams, we adopt maximum ratio transmission (MRT), which is widely chosen for its computational simplicity in cell-free MIMO systems [6], [7]. The MRT precoder at the i -th AP for the k -th user is defined as $\mathbf{p}_{i,k} = \eta_{i,k} \mathbf{w}_{i,k}$, where $\eta_{i,k}^2$ is the transmit power at the i -th AP for the k -th user, and $\mathbf{w}_{i,k} = \frac{\mathbf{h}_{i,k}}{\|\mathbf{h}_{i,k}\|}$.

Next, for radar target sensing, we employ the transmit beampattern metric [1], [3]. At the i -th AP, both information and radar signals are used to detect the target and transmit data simultaneously. Then, the transmit beampattern gain is given by

$$P_i(\theta) = \mathbf{a}^H(\theta) \left(\mathbf{p}_{i,R} \mathbf{p}_{i,R}^H + \mathbf{p}_{i,0} \mathbf{p}_{i,0}^H + \sum_{k=1}^K \mathbf{p}_{i,k} \mathbf{p}_{i,k}^H \right) \mathbf{a}(\theta), \quad \forall i, \quad (4)$$

where $\mathbf{a}(\theta) = [1, e^{j2\pi d_\Delta \sin \theta}, \dots, e^{j2\pi(N-1)d_\Delta \sin \theta}]^T$ represents the steering vector of direction θ with d_Δ being the normalized spacing between consecutive array elements in relation to

the carrier wavelength. Also, we denote the set of angles $\Theta_i = \{\theta_{1,i}, \dots, \theta_{L,i}\}$ where L indicates the number of quantized angles for the target associated with the i -th AP.

The proposed approach aims to guarantee a minimum beampattern gain G_i^{\min} for angles Θ_i at the i -th AP, as in [3]. Note that the angles in the set Θ_i are within the main beam for sensing. Our objective is to maximize the minimum rate of users subject to constraints on a power budget and a minimum beampattern gain for all angles in Θ_i at each AP. This problem is formulated as

$$\max_{\mathbf{p}_{i,0}, \mathbf{p}_{i,R}, \eta_{i,k}, r_k} \min_k r_k + R_k^p \quad (5a)$$

$$\text{s.t. } \sum_{j=1}^K r_j \leq R_k^c, \forall k \quad (5b)$$

$$P_i(\theta_{l,i}) \geq G_i^{\min}, \forall \theta_{l,i} \in \Theta_i, \forall i \quad (5c)$$

$$\mathbf{p}_{i,R}^H \mathbf{p}_{i,R} + \mathbf{p}_{i,0}^H \mathbf{p}_{i,0} + \sum_{k=1}^K \eta_{i,k}^2 \leq P_{i,\max}, \forall i \quad (5d)$$

$$r_k \geq 0, \eta_{i,k} \geq 0, \forall k, \forall i, \quad (5e)$$

where $P_{i,\max}$ represents the maximum power available at the i -th AP, constraint (5b) guarantees that the common stream can be decoded by all users, and (5c) establishes the minimum beampattern gain for the angles associated with the i -th target, which quantifies the spatial distribution of transmit signal power required to satisfy specific sensing requirements. Note that problem (5) is non-convex due to user-coupled SINR expressions in both the objective and the common rate constraint. Thus, we propose an SCA-based approach utilizing tailored surrogate functions to obtain its solution in the following.

III. PROPOSED SCHEME

In this section, we present our proposed solution to the problem (5). First, by introducing an auxiliary variable t , we reformulate the problem (5) as

$$\max_{\mathbf{p}_{i,0}, \mathbf{p}_{i,R}, \eta_{i,k}, r_k} t \quad (6a)$$

$$\text{s.t. } r_k + R_k^p \geq t, \forall k \quad (6b)$$

$$(5b) - (5e). \quad (6c)$$

To develop the proposed SCA-based method, we stack the channels and precoding vectors of all APs for each user and define $\tilde{\mathbf{p}}_0 = [\mathbf{p}_{1,0}^T, \dots, \mathbf{p}_{M,0}^T]^T \in \mathbb{C}^{MN \times 1}$, $\tilde{\mathbf{h}}_k = [\mathbf{h}_{1,k}^T, \dots, \mathbf{h}_{M,k}^T]^T \in \mathbb{C}^{MN \times 1}$, $\tilde{\mathbf{p}}_R = [\mathbf{p}_{1,R}^T, \dots, \mathbf{p}_{M,R}^T]^T \in \mathbb{C}^{MN \times 1}$, $\tilde{\mathbf{w}}_k = [\mathbf{w}_{1,k}^T, \dots, \mathbf{w}_{M,k}^T]^T$, and $\tilde{\boldsymbol{\eta}}_k = [\eta_{1,k}, \dots, \eta_{M,k}]^T \in \mathbb{R}^{M \times 1}$.

In (2) and (3), the term $\left| \sum_{i=1}^M \mathbf{h}_{i,k}^H \mathbf{p}_{i,k} \right|^2$ can be expressed as $|\mathbf{c}_{k,k'}^T \tilde{\boldsymbol{\eta}}_{k'}|^2$ where $\mathbf{c}_{k,k'} = [\mathbf{h}_{1,k}^H \mathbf{w}_{1,k'}, \dots, \mathbf{h}_{M,k}^H \mathbf{w}_{M,k'}]^T$. Also, utilizing the slack variables ω_k and B_k , the minimum rate constraint (6b) can be reformulated to

$$\frac{|\mathbf{c}_{k,k'}^T \tilde{\boldsymbol{\eta}}_{k'}|^2}{B_k} \geq \omega_k - 1, \quad (7a)$$

$$\sum_{k'=1, k' \neq k}^K |\mathbf{c}_{k,k'}^T \tilde{\boldsymbol{\eta}}_{k'}|^2 + |\tilde{\mathbf{h}}_k^H \tilde{\mathbf{p}}_R|^2 + \sigma_k^2 \leq B_k, \quad (7b)$$

$$2^{t-r_k} \leq \omega_k. \quad (7c)$$

Further adding the slack variables ν and C_k , constraint (5b) is transformed into

$$\frac{|\tilde{\mathbf{h}}_k^H \tilde{\mathbf{p}}_0|^2}{C_k} \geq \nu - 1, \quad (8a)$$

$$\sum_{k'=1}^K |\mathbf{c}_{k,k'}^T \tilde{\boldsymbol{\eta}}_{k'}|^2 + |\tilde{\mathbf{h}}_k^H \tilde{\mathbf{p}}_R|^2 + \sigma_k^2 \leq C_k, \quad (8b)$$

$$2^b \leq \nu, \quad (8c)$$

where $b = \sum r_k$. As constraints (7a) and (8a) are still non-convex, we employ a linear lower bound approximation from [10]. An approximation of (7a) is defined as

$$\frac{2\Re\left(\left(\tilde{\boldsymbol{\eta}}_k^{(n)}\right)^T \mathbf{c}_{k,k} \mathbf{c}_{k,k}^T \tilde{\boldsymbol{\eta}}_k^{(n)}\right)}{B_k^{(n)}} - B_k \left(\frac{|\mathbf{c}_{k,k}^T \tilde{\boldsymbol{\eta}}_k^{(n)}|^2}{B_k^{(n)}} \right)^2 \geq \omega_k - 1, \forall k, \quad (9)$$

where $\Re(\cdot)$ denotes the real part of a complex number, and $\{B_k^{(n)}, \tilde{\boldsymbol{\eta}}_k^{(n)}\}$ represents the optimal $\{B_k, \tilde{\boldsymbol{\eta}}_k\}$ obtained at the n -th iteration. Similarly, an approximation of (8a) at the n -th iteration point $(\tilde{\mathbf{p}}_0^{(n)}, C_k^{(n)})$ is given as

$$\frac{2\Re\left(\left(\tilde{\mathbf{p}}_0^{(n)}\right)^H \tilde{\mathbf{h}}_k \tilde{\mathbf{h}}_k^H \tilde{\mathbf{p}}_0^{(n)}\right)}{C_k^{(n)}} - C_k \left(\frac{|\tilde{\mathbf{h}}_k^H \tilde{\mathbf{p}}_0^{(n)}|^2}{C_k^{(n)}} \right)^2 \geq \nu - 1, \forall k. \quad (10)$$

Regarding the approximation of the non-convex constraint (5c) for radar sensing, we adopt the first-order Taylor expansion at a given point $\mathbf{p}_{i,j}^{(n)}$ with $|\mathbf{p}_{i,j}^H \mathbf{a}(\theta)|^2 \geq 2\Re\{\mathbf{a}^H(\theta) \mathbf{p}_{i,j}^{(n)} \mathbf{p}_{i,j}^H \mathbf{a}(\theta)\} - |\left(\mathbf{p}_{i,j}^{(n)}\right)^H \mathbf{a}(\theta)|^2$. Then, by applying the approximation to the remaining terms, constraint (5c) is transformed into

$$\begin{aligned} & 2\Re\{\mathbf{a}^H(\theta_{l,i}) \mathbf{p}_{i,R}^{(n)} \mathbf{p}_{i,R}^H \mathbf{a}(\theta_{l,i})\} - \left| \left(\mathbf{p}_{i,R}^{(n)}\right)^H \mathbf{a}(\theta_{l,i}) \right|^2 \\ & + 2 \sum_{j=0}^K \Re\{\mathbf{a}^H(\theta_{l,i}) \mathbf{p}_{i,j}^{(n)} \mathbf{p}_{i,j}^H \mathbf{a}(\theta_{l,i})\} \\ & - \sum_{j=0}^K \left| \left(\mathbf{p}_{i,j}^{(n)}\right)^H \mathbf{a}(\theta_{l,i}) \right|^2 \geq G_i^{\min}, \forall \theta_{l,i} \in \Theta_i, \forall i. \end{aligned} \quad (11)$$

Therefore, given the initial feasible points $\{\tilde{\mathbf{p}}_0^{(n)}, \tilde{\mathbf{p}}_R^{(n)}, \tilde{\boldsymbol{\eta}}_k^{(n)}, C_k^{(n)}, B_k^{(n)}\}$, problem (5) is expressed as

$$\max_{\nu, t, \{r_k, \mathbf{p}_{i,0}, \mathbf{p}_{i,R}, \eta_{i,k}, \omega_k, B_k, C_k\}} t \quad (12a)$$

$$\text{s.t. } \|\mathbf{p}_{i,0}\|^2 + \|\mathbf{p}_{i,R}\|^2 + \sum_{k=1}^K (\eta_{i,k})^2 \leq P_{i,\max}, \forall i \quad (12b)$$

$$t, r_k, B_k, C_k, \omega_k, \nu \geq 0, \forall k, \forall i, \quad (12c)$$

Problem (12) is convex and can be solved using CVX [18]. At the n -th iteration, given the initial feasible points $\{\tilde{\mathbf{p}}_0^{(n)}, \tilde{\mathbf{p}}_R^{(n)}, \tilde{\boldsymbol{\eta}}_k^{(n)}, C_k^{(n)}, B_k^{(n)}\}$, problem (12) is solved to update the precoding vectors and common rate variables. The updated solution then serves as the new feasible points $\{\tilde{\mathbf{p}}_0^{(n+1)}, \tilde{\mathbf{p}}_R^{(n+1)}, \tilde{\boldsymbol{\eta}}_k^{(n+1)}, C_k^{(n+1)}, B_k^{(n+1)}\}$ for the $(n+1)$ -th iteration. This process is repeated until convergence

The proposed iterative algorithm for problem (5) relaxes the non-convex constraints (7a), (7b), and (5c) using tight convex lower bounds given in (9), (10), and (11), respectively. Then, the solution to problem (12) at the n -th iteration remains feasible at the $(n+1)$ -th iteration. Moreover, given a finite power budget, the objective function is non-decreasing and bounded, ensuring convergence.

IV. NUMERICAL RESULTS

In this section, we present the simulation results to evaluate the performance of our proposed scheme through Monte Carlo simulations averaging over 500 independent channel realizations. The simulation scenario adopts the wrap-around technique where APs and users are randomly distributed in an area of $200 \times 200 \text{ m}^2$. The channel vectors are modeled as $\mathbf{h}_{i,k} = \sqrt{\chi_{i,k}} \tilde{\mathbf{h}}_{i,k}$, where $\tilde{\mathbf{h}}_{i,k}$ indicates Rayleigh fading with $\mathcal{CN} \sim (0, 1)$, and $\chi_{i,k}$ represents the large-scale fading [6]. The noise power is set to $\sigma_k = -94 \text{ dBm}$. The angles $\theta_{l,i} \in \Theta_l$ for the target sensed by the i -th AP are taken from $\theta_i^* - \frac{\pi}{18} \leq \theta_{l,i} \leq \theta_i^* + \frac{\pi}{18}$, where θ_i^* is the azimuth angle of the target based on radar prior knowledge and is assumed to be randomly selected from $[-90^\circ, 90^\circ]$.

To sense the target, the dedicated radar signal s_R can be adopted in (1b). Instead, RSMA can exploit the common stream which can be utilized as a radar sequence, managing communication-radar interference. We will show that the proposed scheme can meet radar sensing requirements without the need for the dedicated radar signal s_R . To investigate the performance loss due to the removal of s_R , we consider two cases in RSMA: “RSMA with s_R ” where a dedicated radar signal is utilized in RSMA, and “RSMA without s_R ” where RSMA operates without the dedicated radar signal and uses the common stream for sensing.

Moreover, we consider the following baseline schemes: “noRSMA” applies ISAC without RSMA, “RSMA without sensing” employs RSMA without sensing capabilities, and “Radar only” in [3] assumes only radar sensing without any users. The noRSMA scheme does not divide the message intended for each user and therefore does not consider both the common stream and the common rate variables. The baseline schemes without sensing capabilities do not include the dedicated radar signal, and the sensing constraint (5c) is removed. The minimum beampattern gain G_{\min} required at the sensing angles of interest is defined as $G_{\min} = \kappa G^*$, where κ equals the relative gain and G^* represents the beampattern gain obtained for the solution of “Radar only”.

Fig. 3 illustrates the max-min rate with respect to κ with $N = 6$, $P_{\max} = 20 \text{ dBm}$ and $M = 3$. We can see the improvement in the proposed scheme compared with the traditional method without RSMA. The reason is mainly due to the capability of RSMA to decode interference by using the common stream. Note that the proposed scheme uses MRT for private precoding, while optimizes the common precoder to manage both inter-user and communication-radar interference. Fig. 4 shows the transmit beampattern for the target associated with the first AP with $K = 9$, $\kappa = 0.9$, and $\theta_1^* = 0^\circ$. We observe that the noRSMA method performs similarly to RSMA, as both satisfy the radar constraint (5c) and allocate remaining resources to maximize user rates. As shown in Fig. 3 and 4, the performance of RSMA with and without the dedicated radar signal is quite similar, showing that removing s_R does not impact on the performance. This observation extends to suboptimal radar schemes, such as conjugate sensing beamforming based on the target’s direction, which is a special case of RSMA with s_R . Thus, we conclude that the proposed scheme works well without the dedicated

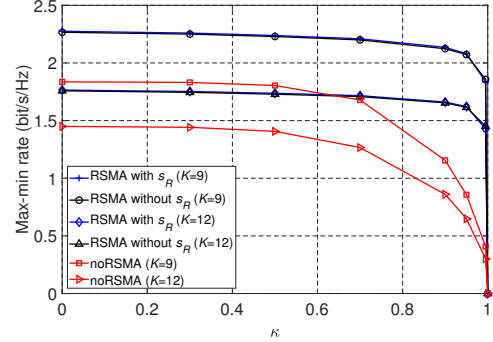


Fig. 3. Max-min rate with respect to κ .

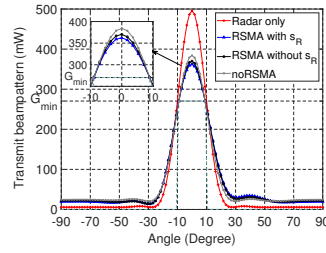


Fig. 4. Transmit beampattern for $\theta_1^* = 0^\circ$. Fig. 5. Convergence behavior of the proposed scheme.

radar signal. Therefore, in the following simulations, we do not consider the dedicated radar signal in RSMA and denote our proposed scheme as “RSMA”.

Fig. 5 presents the convergence behavior of the proposed scheme and traditional methods with $N = 6$, $P_{\max} = 20 \text{ dBm}$, and $\kappa = 0.9$. We can check that the RSMA-based scheme converges within 12 iterations.

As a comparative scheme, we include the NOMA-based method, optimizing the radar precoder and employing MRT and user grouping [19]. Users are grouped into clusters with two users each, applying NOMA within clusters and treating inter-cluster interference as noise. In each cluster, SIC follows a descending decoding order so that the k -th user decodes the messages of all users with indices $u \geq k$. A SIC constraint ensures that the rate allocated to the u -th user’s message does not exceed the rate at which the k -th user can decode it.

Fig. 6 illustrates the max-min rate with respect to the maximum transmission power at each AP with $N = 6$, $K = 6$ and $\kappa = 0.9$. We observe that RSMA achieves a higher max-min rate compared to noRSMA and NOMA due to the common stream which manages interference between sensing and communication, enabling a trade-off between fully decoding the interference and treating it as noise. Furthermore, the proposed RSMA scheme with sensing can achieve similar performance to RSMA without sensing. At high transmission power, the noRSMA method cannot efficiently use the available power due to inter-user interference. The performance of the NOMA-based method is limited by the SIC constraint, which requires that the far user’s rate allocation does not exceed the rate at which the near user can decode the far user’s message.

Fig. 7 shows the max-min rate with respect to the number of APs with $\kappa = 0.9$. For a fair comparison, we set a maximum

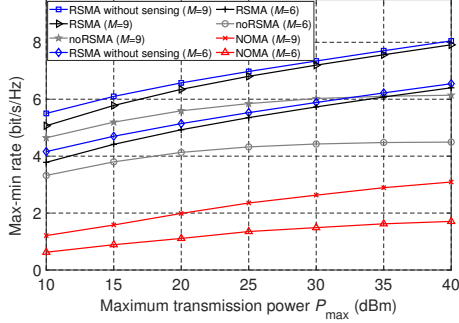


Fig. 6. Max-min rate with respect to the transmission power.

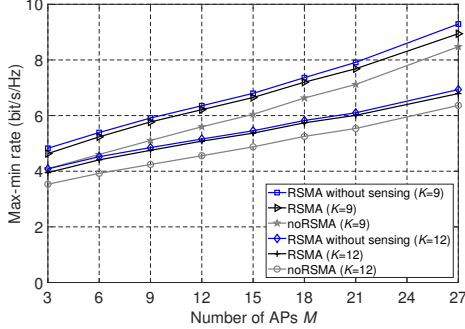


Fig. 7. Max-min rate with respect to the number of APs.

total power as $P_S = 2$ W, while the maximum power of each AP is given by $P_{\max} = P_S/M$. Moreover, we fix the total number of antennas as $N_S = 108$, such that the number of antennas of each AP equals $N = \lfloor N_S/M \rfloor$, where $\lfloor \cdot \rfloor$ represents the floor function. We can see that deploying more APs significantly improves the overall performance because APs can be located closer to users. Similar to Fig. 6, we can check that the proposed scheme with sensing can deliver performance comparable to RSMA without sensing. This indicates that our joint design of RSMA and radar does not sacrifice data rate performance compared to RSMA without sensing capabilities.

The simulations are performed on an Intel Core i9-14900K computer with 64 GB of RAM. We confirm through simulations that RSMA requires almost the same computational complexity compared to the noRSMA while providing a considerable improvement in system performance. The computational complexity of the “RSMA without s_R ” scheme is given by Problem (12), excluding $\mathbf{p}_{i,R}$, and can be expressed as $O(T(MN + MK + 4K + 2)^{3.5})$ [12], where T denotes the number of iterations required for convergence. For the noRSMA scheme, the computational complexity is given by $O(T(MN + MK + 2K + 1)^{3.5})$.

V. CONCLUSION

In this paper, we have proposed a new approach based on RSMA with ISAC in a cell-free massive MIMO system. We aim to maximize the minimum rate of users subject to radar sensing requirements. To this end, we have introduced an SCA-based scheme to optimize the power allocated to the private streams of users and the precoding vectors. Simulation results have validated the superior performance of our proposed

scheme compared to traditional methods. Additionally, we have confirmed that the proposed scheme can provide radar sensing capabilities without impacting the communication performance and demonstrated that the common stream can replace the dedicated radar signal to approximate the beampattern and manage interference between users, as well as that between radar and communication.

REFERENCES

- [1] F. Liu, C. Masouros, A. Li, H. Sun, and L. Hanzo, “MU-MIMO Communications with MIMO Radar: From Co-Existence to Joint Transmission,” *IEEE Trans. Wireless Commun.*, vol. 17, no. 4, pp. 2755–2770, Apr. 2018.
- [2] X. Liu, T. Huang, N. Shlezinger, Y. Liu, J. Zhou, and Y. C. Eldar, “Joint Transmit Beamforming for Multiuser MIMO Communications and MIMO Radar,” *IEEE Trans. Signal Process.*, vol. 68, pp. 3929–3944, Jun. 2020.
- [3] H. Hua, J. Xu, and T. X. Han, “Optimal Transmit Beamforming for Integrated Sensing and Communication,” *IEEE Trans. Veh. Technol.*, vol. 72, no. 8, pp. 10588–10603, Aug. 2023.
- [4] Q. Shi, T. Zhang, X. Yu, X. Liu, and I. Lee, “Waveform designs for joint radar-communication systems with OQAM-OFDM,” *Signal Process.*, vol. 195, p. 108462, Jun. 2022.
- [5] F. Zhang, T. Mao, R. Liu, Z. Han, S. Chen, and Z. Wang, “Cross-Domain Dual-Functional OFDM Waveform Design for Accurate Sensing/Positioning,” *IEEE J. Sel. Areas Commun.*, vol. 42, no. 9, pp. 2259–2274, Sep. 2024.
- [6] H. Q. Ngo, A. Ashikhmin, H. Yang, E. G. Larsson, and T. L. Marzetta, “Cell-free massive MIMO versus small cells,” *IEEE Trans. Wireless Commun.*, vol. 16, no. 3, pp. 1834–1850, Mar. 2017.
- [7] H. Q. Ngo, L.-N. Tran, T. Q. Duong, M. Matthaiou, and E. G. Larsson, “On the Total Energy Efficiency of Cell-Free Massive MIMO,” *IEEE Trans. Green Commun. Netw.*, vol. 2, no. 1, pp. 25–39, Mar. 2018.
- [8] E.-K. Hong, I. Lee, B. Shim, Y.-C. Ko, S.-H. Kim, S. Pack, K. Lee, S. Kim, J.-H. Kim, Y. Shin, Y. Kim, and H. Jung, “6G R&D vision: Requirements and candidate technologies,” *J. Commun. Netw.*, vol. 24, no. 2, pp. 232–245, Apr. 2022.
- [9] N. Ghiasi, S. Mashhadi, S. Farahmand, S. M. Razavizadeh, and I. Lee, “Energy Efficient AP Selection for Cell-Free Massive MIMO Systems: Deep Reinforcement Learning Approach,” *IEEE Trans. Green Commun. Netw.*, vol. 7, no. 1, pp. 29–41, Mar. 2023.
- [10] Y. Mao, B. Clerckx, and V. O. K. Li, “Rate-Splitting for Multi-Antenna Non-Orthogonal Unicast and Multicast Transmission: Spectral and Energy Efficiency Analysis,” *IEEE Trans. Commun.*, vol. 67, no. 12, pp. 8754–8770, Dec. 2019.
- [11] B. Clerckx et al., “A Primer on Rate-Splitting Multiple Access: Tutorial, Myths, and Frequently Asked Questions,” *IEEE J. Sel. Areas Commun.*, vol. 41, no. 5, pp. 1265–1308, May 2023.
- [12] M. R. Camana, C. E. Garcia, and I. Koo, “Rate-Splitting Multiple Access in a MISO SWIPT System Assisted by an Intelligent Reflecting Surface,” *IEEE Trans. Green Commun. Netw.*, vol. 6, no. 4, pp. 2084–2099, Dec. 2022.
- [13] C. Xu, B. Clerckx, S. Chen, Y. Mao, and J. Zhang, “Rate-Splitting Multiple Access for Multi-Antenna Joint Radar and Communications,” *IEEE J. Sel. Topics Signal Process.*, vol. 15, no. 6, pp. 1332–1347, Nov. 2021.
- [14] L. Yin, Y. Mao, O. Dizdar, and B. Clerckx, “Rate-Splitting Multiple Access for 6G—Part II: Interplay With Integrated Sensing and Communications,” *IEEE Commun. Lett.*, vol. 26, no. 10, pp. 2237–2241, Oct. 2022.
- [15] A. Mishra, Y. Mao, L. Sanguinetti, and B. Clerckx, “Rate-Splitting Assisted Massive Machine-Type Communications in Cell-Free Massive MIMO”, *IEEE Commun. Lett.*, vol. 26, no. 6, pp. 1358–1362, Jun. 2022.
- [16] J. Zheng, J. Zhang, J. Cheng, V. C. M. Leung, D. W. K. Ng, and B. Ai, “Asynchronous Cell-Free Massive MIMO With Rate-Splitting,” *IEEE J. Sel. Areas Commun.*, vol. 41, no. 5, pp. 1366–1382, May 2023.
- [17] W. Mao, Y. Lu, C.-Y. Chi, B. Ai, Z. Zhong, and Z. Ding, “Communication-Sensing Region for Cell-Free Massive MIMO ISAC Systems,” *IEEE Trans. Wireless Commun.*, vol. 23, no. 9, pp. 12396–12411, Sep. 2024.
- [18] M. C. Grant and S. P. Boyd. “CVX: MATLAB Software for Disciplined Convex Programming, Version 2.2.” Jul. 2024. [Online]. Available: <http://cvxr.com/cvx>
- [19] J. Zhang, J. Fan, J. Zhang, D. W. K. Ng, Q. Sun, and B. Ai, “Performance Analysis and Optimization of NOMA-Based Cell-Free Massive MIMO for IoT,” *IEEE Internet Things J.*, vol. 9, no. 12, pp. 9625–9639, Jun. 2022.